# Pre-oxidation coupled with ceramic membrane filtration for natural organic matter removal and membrane fouling mitigation during surface water treatment

Keying Li[a], Yong Wei[a,b,*], Ming Kong[c,*], Ziyin Guo[b], Zhengbo Luo[b], Xianjian Li[a], Rongkai Shi[a]

[a]*School of Urban Construction, Changzhou University, Changzhou 213164, China, emails: weiyong@cczu.edu.cn (Y. Wei), 2894613425@qq.com (K.Y. Li), 1397879511@qq.com (X.J. Li), 3119561783@qq.com (R.K. Shi)*
[b]*School of Environmental Science and Engineering, Changzhou University, Changzhou 213164, China, emails: 2820960776@qq.com (Z.Y. Guo), 346151446@qq.com (Z.B. Luo)*
[c]*Nanjing Institute of Environmental Sciences, Ministry of Ecology and Environment, Nanjing 210042, China, email: kongming@nies.org (M. Kong)*

## ABSTRACT

Catalytic ozonation coupled with membrane filtration has been widely used in water treatment to improve effluent quality as well as control membrane fouling. In this study, the removal of natural organic matter (NOM) from surface water and the mitigation of membrane fouling by $O_3/H_2O_2/TiO_2$ pre-oxidation coupled with ceramic membrane in static cycling model were investigated. The results showed that the pre-oxidation of $O_3$, $O_3/H_2O_2$ and $O_3/TiO_2$ significantly improved the removal rate of NOM, with the sequence of $O_3/TiO_2 > O_3/H_2O_2 > O_3$. Under the $O_3/TiO_2$ pre-oxidation, the macromolecular substances such as aromatic proteins, fulvic acid-like and humic-like substances were completely removed, which may be due to the accelerated ozonolysis and $^•OH$ formation by $TiO_2$. Meanwhile, three-dimensional fluorescence spectra and molecular weight distribution showed that humic acids and biopolymers were the main pollutants, and also the main causes for membrane fouling. The pre-oxidation of $O_3$, $O_3/H_2O_2$ and $O_3/TiO_2$ significantly mitigated the membrane fouling via the degradation of humic acids and biopolymers with the order of $O_3/TiO_2 > O_3/H_2O_2 > O_3$. Under the optimal pretreatment, the resistance of membrane fouling was significantly reduced, and the transmembrane pressure (TMP) decreased by 62.2%. Redundancy analysis showed that the molecular weight was the most important factor for total fouling resistance, while turbidity was negatively correlated with the fouling resistance. In addition, the $O_3/H_2O_2/TiO_2$ pretreatment can also enhance NOM removal and membrane fouling mitigation under long-term (48 h) cycle model.

*Keywords:* Pre-oxidation; Ceramic membrane; Surface water; Natural organic matter; Membrane fouling

## 1. Introduction

The quality of surface waters, especially for the drinking water, had been seriously polluted in many areas in recent years. Natural organic matter (NOM) has been reported to be one of the most prevalent compounds in aquatic ecosystems, with the average concentrations ranging from a few mg/L to hundreds of mg/L [1]. NOM was characterized with complex compositions which can significantly influence the quality of natural waters [2]. The specific fractions of NOMs, such as humic acid (HA) and fulvic acid (FA), has strong complexation ability with heavy

---

* Corresponding authors.

metals, which significantly affect the transportation, bio-availability and toxicity of those metals [3]. In addition, a series of disinfection by-products can be produced as the raw water containing NOM was treated with disinfectants [4], which posed a serious threat to human health. In addition, presence of NOM could increase the amount of water treatment agents as well as reduce treatment efficiency. Therefore, the removal of NOM from surface water receives increasing attentions in recent years.

Conventional methods for NOM removal include coagulation/flocculation/precipitation, activated carbon adsorption, advanced oxidation process (AOP), etc. [5]. Among them, the coagulants have been widely used in NOM removal. For example, NOM was removed by 50%~60% after the treatment with high dosage of coagulants [6]. Lee et al. [7] used different doses of biochar to adsorb the aromatic organics from the river waters and the overall adsorption capacity was 6.4 mg-DOC/g-C. However, the coagulants and adsorbents were characterized with high sludge yield and cost. In contrast, AOP exhibits the advantages of thorough decomposition of organic matter, high degradation efficiency and absence of secondary fouling. During AOP process, the reactive oxygen species (ROS) such as hydroxyl radicals ($^{\bullet}OH$) were generated. The high oxidation capacity of ROS can enable AOP to achieve complete oxidation or mineralization of organic pollutants under ideal conditions. It was shown that, even though part of NOM was oxidized and decomposed into low molecular weight organic matter [8], AOP usually exhibited a mineralization rate of about 30%–90% [9,10]. Among them, ozone ($O_3$) was a widely used oxidant, which had been widely used for the degradation of NOM and organic pollutants. However, due to the relatively low $^{\bullet}OH$ concentration, hydrogen peroxide and catalyst were usually added to form catalytic ozonation. For example, Tubić et al. [11] explored the effect of different $O_3$/$H_2O_2$ ratios on the removal of NOM in Serbian groundwater and found that the removal efficiency increased with increasing $O_3$/$H_2O_2$ ratio.

In recent decades, membrane filtration technology had received increasing attentions, while a single membrane filtration procedure can not completely remove the NOM. It was reported that the NOM trapped in nanofiltration membrane could reach about 80%, and NOM and other pollutants accumulating on the surface and inside of the membrane resulted in membrane fouling [12]. Pretreatment and some coupled processes could effectively improve NOM removal efficiency and mitigate membrane fouling. For instance, Deng et al. [13] found that the removal rates of $UV_{254}$ and dissolved organic carbon (DOC) for coagulation coupled with membrane filtration were 65% higher than the uncoupled techniques. Zhou et al. [14] coupled nanometer MgO with microfiltration membrane to remove NOM and a total of 92% removal efficiencies were obtained. Cheng et al. [15] found that when 4.0 mg/L $O_3$ was added, the total fouling index of humic acid, sodium alginate and river waters decreased by 39%, 78% and 42%, respectively, and 9 mg/L of $O_3$ pretreatment could remove 35.5% of biopolymer [16]. These results indicated that the pre-ozonation coupled with membrane filtration could effectively degrade NOM and mitigate membrane fouling. However, excessive ozone might damage the filtration

performance of polymer membrane by changing its physical and chemical properties, such as surface charge, surface hydrophilicity and pore size [17]. Therefore, it was necessary to enhance the material of filtration membrane in long-term operation, and inorganic ceramic membrane was a possible choice. Compared with polymeric membrane, the ceramic membrane exhibited many advantages, including robust mechanical, thermal and chemical stability, long service life and high hydrophilicity [18,19], and strong antifouling ability [20]. For example, Tang et al. [21] coupled ozonation with ceramic membrane and found that when ozone dosage was 5 mg/L, the TMP and cake layer resistance reduced by 55.6% and 61.5%, respectively.

In this study, an $O_3$/$H_2O_2$/$TiO_2$ pre-oxidation system was used to enhance the degradation of NOM in surface water as well as to mitigate the membrane fouling. The regional components of three-dimensional fluorescence and the effect of different pre-oxidation on the mitigation of membrane fouling were analyzed. Redundancy analysis (RDA) was used to reveal the correlation among different MOM parameters, removal efficiencies and membrane fouling resistance. Results obtained are of great significance to guide the practical application of membrane technology in the removal of NOM from surface water.

## 2. Materials and methods

### 2.1. Reagents and surface water

$H_2O_2$ (30%, Analytical Pure), nano-$TiO_2$ P25 (Degussa, particle size of 20 nm, surface area of 50 m²/g), NaOH (Analytical Pure), NaClO (Analytical Pure), and ozone generator (XZY-DMN-5G, Anhui) were obtained based on the previous methods. Surface water was taken from Lake Ruoyu, Wujin Campus of Changzhou University, and filtered by sand filter tank to remove the suspended particles. The physico-chemical properties of water samples were as follows: pH: 7.5, turbidity: 0.4 NTU, total organic carbon (TOC): 4.84 mg/L, $UV_{254}$: 0.069 cm⁻¹, and specific ultraviolet absorbance (SUVA): 1.43 L/mg·m.

### 2.2. Experimental setup and operation

The total volume of membrane reactor was about 50 L, with the size of 300 mm (length) × 300 mm (width) × 600 mm (height) (Fig. 1). Baffles were used to separate the reactor into 25 L of pre-oxidation reaction zone and 25 L of ceramic membrane pool zone. Static circulation model was employed in the experiment. Prior to the reaction, 1.4~2 mg/L of $O_3$ and 0.029 mmol/L of $H_2O_2$ or 1 g/L of $TiO_2$ catalysts were added into the raw water. The electric stirrer (JJ-1A, Changzhou, Jiangsu) was conducted with a speed of 400 rpm to ensure the complete mixture. The pretreated waters were firstly entered into the membrane pool area, and the ceramic diaphragm was pumped with negative pressure by peristaltic pump to circulate the water back to the pre-oxidation reaction area. The pump was operated with a model of 8 min (on): 2 min (off). A pressure sensor (MIK-P300, Hangzhou, Zhejiang) was installed between the ceramic membrane and the peristaltic pump to measure the TMP, which was transported to the computer for data analysis via a paperless
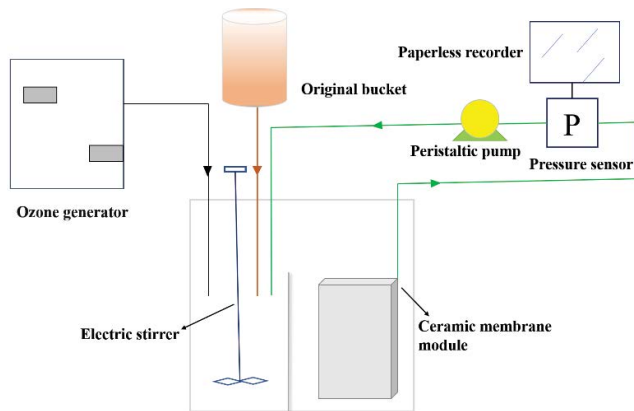
Fig. 1. $O_3/H_2O_2/TiO_2$ pretreatment coupled with ceramic membrane.

recorder (MIK-R200T, Hangzhou, Zhejiang). The characteristic parameters for the ceramic membrane were as follows: material: $Al_2O_3$, average pore size: 0.1 μm, filtration area: 0.05 m², pure water flux: 0.025 m³/m²·h. Under the same experimental conditions, the other four parallel filtration experiments, including single ceramic membrane filtration (CMF), $O_3$ pre-oxidation/membrane filtration ($O_3$-CMF), $O_3/H_2O_2$ pre-oxidation/membrane filtration ($O_3/H_2O_2$-CMF) and $O_3/TiO_2$ pre-oxidation/membrane filtration ($O_3/TiO_2$-CMF), were carried out simultaneously.

## 2.3. Analytical methods

### 2.3.1. Determination of water samples

The water sample was filtered by 0.45 μm microfiltration membrane before determination. The TOC was determined by total organic carbon analyzer (multiN/C2100, Jena, Germany), and ultraviolet (UV) absorbance at 254 nm was measured by UV-Visible spectrophotometer (IS5, Shanghai, China). The turbidity was determined by turbidity meter (TDT-1, Wuhan, China).

### 2.3.2. Three-dimensional fluorescence spectrum

Fluorescence excitation–emission matrices (EEM) were measured using a fluorescence spectrophotometer (Cary Eclipse, Shanghai, China), with excitation spectra (Ex) from 220 to 400 nm in 5 nm increments and emission spectra (Em) from 280 to 550 nm in 2 nm increments. The five regions of EEM spectrum can be divided into region I (Ex/Em: 220–250/280–330 nm), region II (Ex/Em: 220–250/330–380 nm) (aromatic proteins), region III (Ex/Em: 220–250/380–480 nm) (fulvic acid-like substances), region IV (Ex/Em: 250–440/280-380 nm) (soluble microbial products (SMP)), and region V (Ex/Em: 250–400/380–540 nm) (humic-like substances) [22]. Matlab R 2022a was used for fluorescence regional integration (FRI) analysis of EEM spectra data. The Rayleigh and Raman scattering were deducted by trigonometric difference method, and the fluorescence integral of each sample can be obtained.

### 2.3.3. Molecular weight distribution

The molecular weight (MW) distribution of water samples was determined using high performance gel chromatography (HPSEC) combined with on-line UVA (LC-UV, 254 nm) and DOC detection (LC-DOC). The mobile phase was composed of silica gel column and phosphate buffer solution (0.008 mol/L of $Na_2HPO_4$ and 0.018 mol/L of $KH_2PO_4$). The flow rate and column temperature were 0.6 mL/min and 30°C, respectively. The standard sodium polystyrene sulfonate was used to calibrate the MW distribution of water samples.

### 2.3.4. Membrane cleaning procedures and fouling resistance

After each filtration, the fouled ceramic membrane was cleaned with physical and chemical methods. The steps included: (1) Firstly, the diaphragm was sponged and rinsed with pure water to remove reversible membrane fouling such as filter cake layer on the membrane surface and then emptied; (2) The ceramic membrane was hydraulically backwashed with 72 L/(m²·h) constant current for 90 s; (3) The ceramic membrane was soaked in 0.01 mol/L of NaOH and 0.01 mol/L of NaClO mixture for 5 h.

In order to evaluate the effect of pre-oxidation on membrane fouling mitigation, the Darcy's law and series resistance model were used to calculate membrane fouling resistance [23]. Reversible fouling resistance was the difference between the resistance before and after physical cleaning, while the irreversible fouling resistance was those between the resistance before and after chemical cleaning.

$$R = \frac{TMP}{\mu J} = R_m + R_{ir} + R_r \tag{1}$$

where TMP is the trans membrane pressure (Pa), μ is the viscosity of water at 25°C ($0.8949 \times 10^{-3}$ N·s/m²), $J$ is the osmotic flux (L/h·m²), $R$, $R_m$, $R_{ir}$ and $R_r$ are the total fouling resistance, membrane resistance, irreversible fouling resistance and reversible fouling resistance, respectively.

The total fouling resistance was calculated according to Eq. (2).

$$R = \frac{TMP}{\mu J_1} \tag{2}$$

where $R$ is the total fouling resistance at the end of filtration, and $J_1$ is the osmotic flux at the end of filtration.

The resistance of propria membrane was calculated according to Eq. (3).

$$R_m = \frac{TMP}{\mu J_2} \tag{3}$$

where $R_m$ is the resistance of membrane calculated by cyclic filtration of ultra-pure water, and $J_2$ is the osmotic flux filtered by ultra-pure water.

The reversible fouling resistance could be calculated according to Eq. (4).

$$R_r = \frac{\text{TMP}}{\mu J_1} - \frac{\text{TMP}}{\mu J_3} \qquad (4)$$

where $R_r$ is the reversible fouling resistance which is the difference between the resistance before and after physical cleaning, and $J_3$ is the osmotic flux of filtered ultra-pure water.

When $R_m$ and $R_r$ were measured, the irreversible fouling resistance was calculated according to Eq. (5).

$$R_{ir} = R - R_m - R_r \qquad (5)$$

where $R_{ir}$ is the irreversible fouling resistance which is the difference of resistance before and after chemical cleaning.

### 2.3.5. Membrane fouling analysis

Due to the slight membrane fouling during the 12 h of short-term operation, the 48 h of batch experiment at 54 L/(m²·h) membrane flux was applied to investigate the membrane fouling, which was further evaluated via using scanning electron microscopy (SEM) (JSM-IT100, Japan), Energy dispersive X-ray spectroscopy (EDX) (DRY SD, Japan) and Fourier-transform infrared (FTIR) (Nicolet IS5, USA).

### 2.3.6. RDA analysis

The correlation between membrane fouling resistance (total resistance, reversible resistance and irreversible resistance) and influent characteristics ($UV_{254}$, TOC, SUVA, turbidity, EEM, MW) was analyzed by RDA method. The RDA was analyzed via a linear model in which seven different influent parameters were set as explanatory variables and three membrane fouling resistance as response variables. The significance level of each explanatory variable to the response variables was evaluated by Monte Carlo permutation test. All data were analyzed using Canoco5 software.

## 3. Results and discussion

### 3.1. Enhanced NOM removal by pre-oxidation coupled with ceramic membrane

In this study, CMF was used as the control, and three oxidation systems and three pre-oxidation: $O_3$ oxidation (1.4~2 mg/L dosage), $O_3/H_2O_2$ oxidation (1.4~2 mg/L of $O_3$ + 0.029 mmol/L of $H_2O_2$), and $O_3/TiO_2$ oxidation (1.4~2 mg/L of $O_3$ + 1 g/L of $TiO_2$) coupled with ceramic membrane were adopted, with the results in Fig. 2. The values of $UV_{254}$, TOC and SUVA in effluent decreased significantly after the application of $O_3$, $O_3/H_2O_2$ and $O_3/TiO_2$ oxidation alone. The removal rates of $UV_{254}$ and TOC values by $O_3/TiO_2$ oxidation was 82% and 46%, respectively, which was 16% and 6% higher than that of $O_3$ oxidation, and 4% and 4% higher than that of $O_3/H_2O_2$ oxidation, which indicated that the pre-oxidation could significantly degrade the NOM. As seen in Fig. 2a, after 12 h of filtration, only 7% of $UV_{254}$ and 20% of TOC could be removed, which indicated that the removal efficiencies for single CMF was limited, while the removal rates of $UV_{254}$ and TOC increased to 78% and 42% after 12 h filtration of $O_3$-CMF, indicating that

ozone could significantly degrade the organic matters. The main reason was that $O_3$ exhibited strong oxidation ability which could directly oxidize the double bonds and specific functional groups of aromatic rings [24].

After $O_3/H_2O_2$-CMF filtration for 12 h, the removal rates of $UV_{254}$ and TOC were 83% and 45%, respectively, which were slightly higher than that of $O_3$-CMF. Although both $H_2O_2$ and $O_3$ can directly degrade the organic matters, the co-existence of $H_2O_2$ can promote $O_3$ to produce more •OH, thus accelerating NOM degradation [25]. Previous studies compared the removal of ofloxacin by $O_3$ and $O_3/H_2O_2$ treatments and found that the removal rate increased from 30% to 55% due to the $H_2O_2$ enhanced $O_3$ decomposition and •OH formation [26].

After 12 h of filtration with $O_3/TiO_2$-CMF, the removal rates of $UV_{254}$ and TOC were 86% and 47%, respectively, which were slightly higher than that of $O_3/H_2O_2$-CMF, demonstrating that $O_3/TiO_2$ pre-oxidation was the most effective procedure for NOM removal. The possible mechanisms for $O_3/TiO_2$ pre-oxidation may be: (1) ozone molecules were adsorbed on the catalyst surface and decomposed into •OH; (2) organic compounds were adsorbed on the catalyst surface and reacted with the adsorbed ozone molecules; (3) ozone molecules and organic compounds were both adsorbed on the catalyst surface which enhanced the catalytic reactions [27].

However, compared with the $UV_{254}$, the pre-oxidation coupled with ceramic membrane exhibited a lower removal efficiency for TOC, with the highest removal efficiency of only 47%. This may be due to the fact that the pre-oxidation can oxidize macromolecular organic substances such as humic acids into small molecular substances, but cannot completely mineralize into carbon dioxide and water. As seen in Fig. 2c, the $UV_{254}$ value decreased faster than that of TOC, resulting in decreased SUVA values. In addition, the turbidity of effluent waters for all systems was <0.01 NTU (Fig. 2d), which demonstrated that the ceramic membrane exhibited a good retention performance for suspended particles.

### 3.2. Effect of pre-oxidation coupled with ceramic membrane on NOM properties

#### 3.2.1. EEM spectrum

The EEM spectra of different treatment systems are shown in Fig. 3. As shown, 5 fluorescence peaks were observed in the raw water samples, indicating the presence of aromatic proteins, fulvic acid-like substances, SMP and humic-like substances. As shown in Table 1, the fluorescence intensities of peaks I-V were 1,941; 1,843; 6,588; 10,402 and 32,529, respectively, showing that the fulvic acid-like substances, SMP and humic-like substances were the main substances. In addition, the peak intensities for CMF decreased to 909; 1,318; 4,196; 7,149 and 16,314, respectively, demonstrating the limited retention for NOM removal. However, after the other pretreatments, the peak intensities decreased significantly (Fig. 3c–e), which indicated that application of the pretreatment can effectively degrade the organic matters. For instance, the peak intensities decreased by more than 80% with the application of $O_3$ and/or $O_3/H_2O_2$ pretreatments, while they were even disappeared after $O_3/TiO_2$
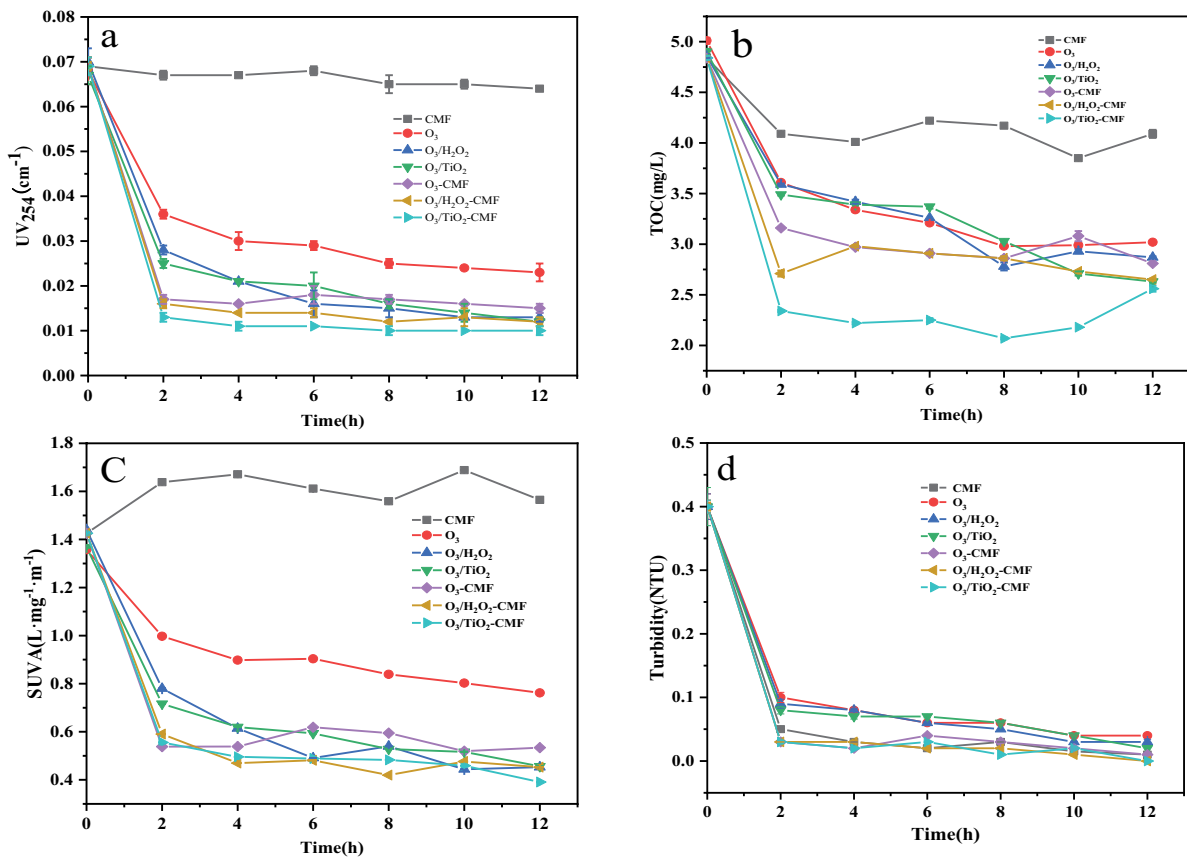
Fig. 2. Effect of different pretreatment coupled with ceramic membranes on NOM removal. (a) $UV_{254}$, (b) TOC, (c) SUVA, and (d) turbidity.

pretreatment showing the complete removal. Similar results can be also found in previous studies demonstrating the efficient removal of organic matters in various systems [28].

### 3.2.2. Molecular weight distribution

In order to investigate the effect of different systems on NOM removal, the LC-TOC and LC-UV were employed to determine the apparent MW distribution. As shown in Fig. 4a, the untreated surface water included three main peaks, representing biopolymers (20,000–200,000 Da), humic substances (350–20,000 Da), and low molecular weight organics (<350 Da) [29]. It was obvious that the biopolymers and humus substances were the main substances. After filtration by CMF, there was no significant difference in the peak intensity of humic substances, demonstrating the limited retention of humic substances by CMF. However, the peak intensities of biopolymer decreased significantly, which indicated that the CMF could remove the high molecular weight organics. With the addition of $O_3$, $O_3/H_2O_2$ and $O_3/TiO_2$ pretreatments, the peak intensities of humic substances and biopolymers decreased significantly, while some low molecular weight organic compounds appeared. The decreased peak intensities of humic substances and biopolymers can be ascribed to the electrophilic interaction of ozone with the specific functional groups such as double bonds and aromatic rings of organic compounds [30]. As for the LC-TOC

chromatography, the peak intensities of both biopolymers and low molecular weight organic compounds were not detected (Fig. 4b), while those of humic substances can be clearly observed. After each pretreatment, the peak intensities of humic substances gradually decreased due to the formation of the free radical [31]. Overall, the $O_3/TiO_2$ pretreatment exhibited the highest effects for NOM removal, which was consistent with the previous studies (Fig. 2).

### 3.3. Effect of pre-oxidation on membrane fouling

#### 3.3.1. Critical membrane flux

The common critical flux measurement methods include flux ladder method, mass conservation method, working curve plotting method, direct observation method and pressure ladder method [32,33]. In this study, the flux step method (constant flux method) was used to measure the membrane flux. After the membrane was operated for a period of time $\Delta t$ (no less than 30 min), the changes of the TMP in $\Delta t$ were observed. If the TMP remained stable, the peristaltic pump was used to adjust the flow rate to obtain a higher membrane flux, and the changes of TMP in $\Delta t$ were measured again. If TMP increased over time, the critical membrane flux was considered to be located between the two membrane fluxes. In this experiment, changes in TMP after 12 h of filtration under three membrane fluxes of 30,
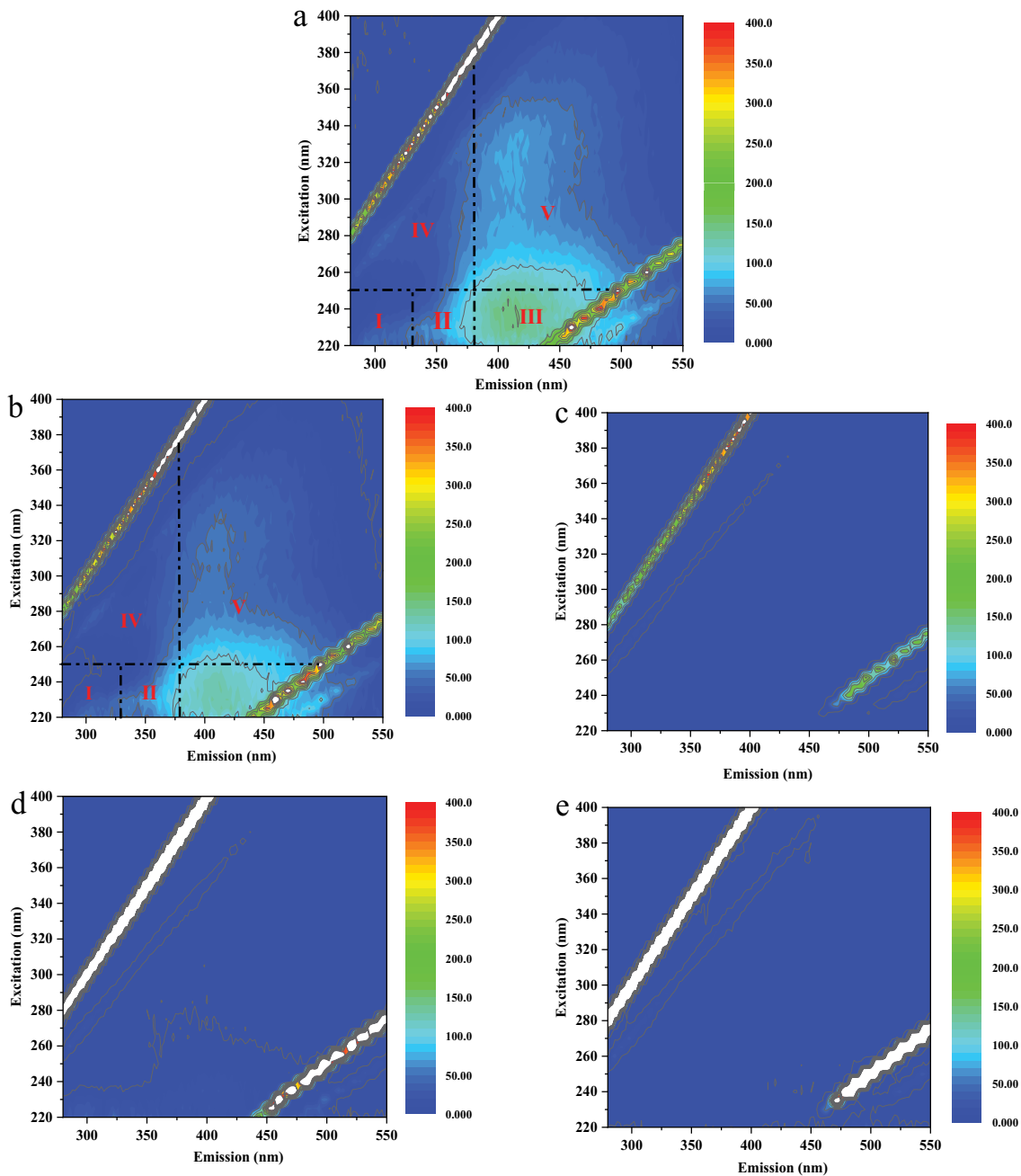
Fig. 3. Effect of different pretreatments on NOM fluorescence characteristics. (a) Raw water, (b) CMF, (c) $O_3$-CMF, (d) $O_3/H_2O_2$-CMF, and (e) $O_3/TiO_2$-CMF.

42 and 54 L/(m²·h) are shown in Fig. 5. The TMP increased with increasing membrane flux, demonstrating that the membrane fouling was significantly enhanced as the membrane flux increased. The 42 L/(m²·h) was thus used as the critical membrane flux, while the higher membrane flux, that is, 54 L/(m²·h), was used in the following studies to explore the effect of pre-oxidation of membrane fouling mitigating.

### 3.3.2. Effect of different pre-oxidation on membrane fouling

When the membrane flux was 54 L/(m²·h) (45.08 L/min), the TMP and the membrane fouling resistance of

Table 1
Fluorescence integrals of each region

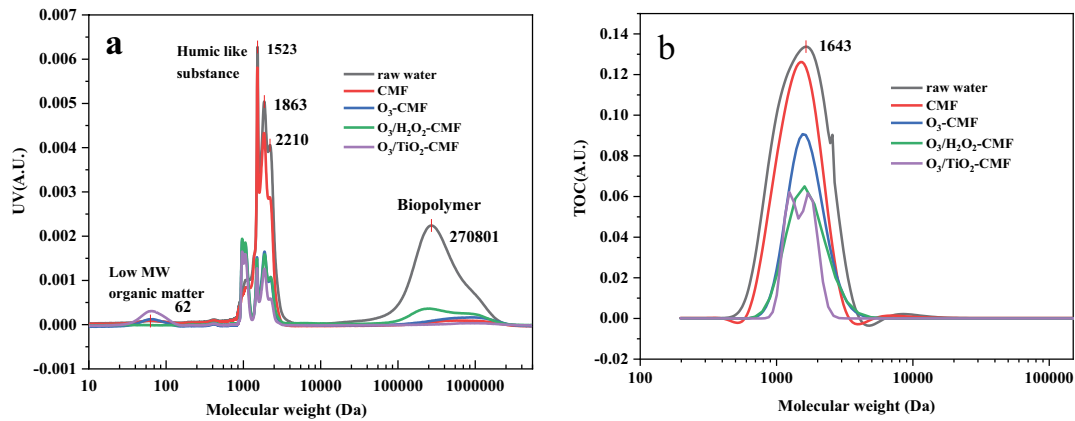| Region Technology | I | II | III | IV | V |
|---|---|---|---|---|---|
| Raw water | 1,941 | 1,843 | 6,588 | 10,402 | 32,529 |
| CMF | 909 | 1,318 | 4,196 | 7,149 | 16,314 |
| $O_3$-CMF | 125 | 21 | 0 | 4,719 | 2,256 |
| $O_3/H_2O_2$-CMF | 63 | 0 | 11 | 5,582 | 1,339 |
| $O_3/TiO_2$-CMF | 0 | 0 | 0 | 26 | 0 |

Fig. 4. Molecular weight distribution of NOM in raw water, CMF, $O_3$-CMF, $O_3/H_2O_2$-CMF, $O_3/TiO_2$-CMF. (a) LC-UV and (b) LC-TOC.
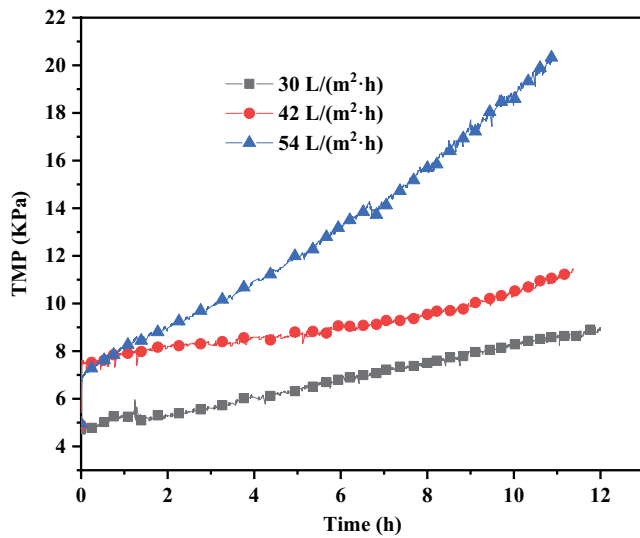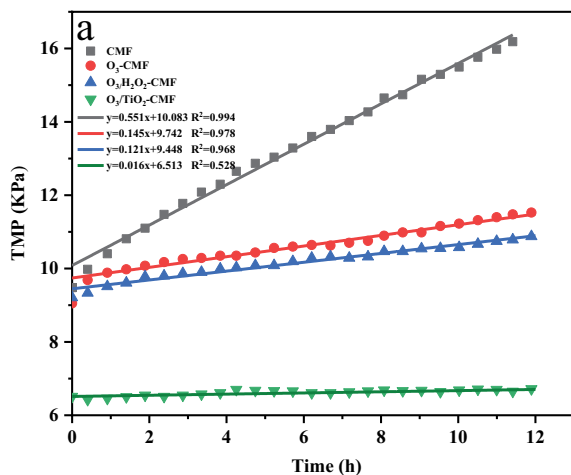


Fig. 5. Effects of different membrane fluxes on transmembrane pressure.

four filtration systems were used for comparative analysis. As shown, the TMP gradually increased with increasing running time. When CMF alone was run for 12 h, TMP increased by 9 KPa and the total resistance of membrane fouling reached $1.482 \times 10^{12}$ m$^{-1}$. The main reason may be due to the deposition on the membrane surface and membrane pore blockage of organic matters. The TMP of $O_3$-CMF, $O_3/H_2O_2$-CMF, and $O_3/TiO_2$-CMF was low and exhibited a little change with running time, which indicated that pre-oxidation could effectively mitigate membrane fouling [34,35], especially for the $O_3/TiO_2$-CMF treatment. Chen et al. [36] also found that both ozone and catalytic ozone could mitigate membrane fouling, and the higher membrane flux in the $O_3/TiO_2$-CMF treatment mainly be due to the enhanced conversion of ozone into •OH.

As shown in Fig. 6b, high membrane fouling resistance, including membrane inherent resistance, reversible fouling resistance and irreversible fouling resistance, was observed for the CMF treatment, while the pre-oxidation could mitigate the fouling resistance, with the order of $O_3/TiO_2 > O_3/H_2O_2 > O_3$. pre-oxidation can simultaneously reduce
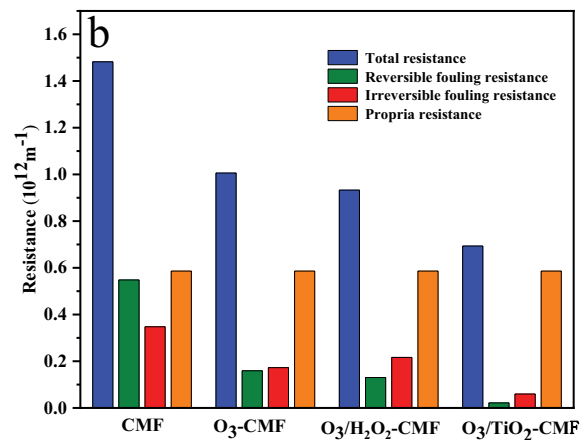


Fig. 6. Influence of different pre-oxidation on membrane fouling. (a) Transmembrane pressure filtered by different pre-oxidation coupled ceramic membranes for 12 h and (b) membrane fouling resistance filtered by different pre-oxidation coupled ceramic membranes.

reversible fouling resistance (about 90%) and irreversible fouling resistance (about 60%). Obviously, the mitigation of irreversible fouling resistance was relatively low, so the proportion of irreversible fouling increased after pre-oxidation. Some hydrophobic macromolecules were oxidized to small molecules, resulting in mitigating reversible fouling resistance [37]. In addition, the small hydrophilic organic matter generated by pre-oxidation may block the membrane pore and cause irreversible fouling [38].

### 3.3.3. Cleaning solution analysis of membrane fouling

The $UV_{254}$, TOC and EEM of chemical cleaning solution under four operation conditions are shown in Figs. 7 and 8. As shown, obvious aromatic proteins and fulvic acid-like substances could be seen in the cleaning solution of CMF system (Fig. 7a), while the fluorescence intensities of all peaks decreased significantly due to the application of $O_3$, $O_3/H_2O_2$ and $O_3/TiO_2$ pretreatments (Fig. 7b–d), which indicated that pre-oxidation could effectively mitigate membrane fouling Variations in $UV_{254}$ and TOC among different treatments also indicated that pre-oxidation could effectively mitigate the membrane fouling and $O_3/TiO_2$ pretreatment exhibited the highest removal efficiencies (Fig. 8), which was consistent with previous results (Fig. 6).

### 3.4. Long-term membrane fouling

Under the same operate condition, the experimental setup with different filtration models were run in batch for 48 h, and the ceramic membrane was characterized by SEM, energy-dispersive X-ray spectroscopy (EDS) and FTIR to further reveal the membrane fouling.

As shown in Fig. 9, the surface of the clean ceramic membrane was porous, while a thick layer of pollutants was covered due to the 48 h of filtration by CMF (Fig. 9a–c). After $O_3/TiO_2$-CMF filtration for 48 h, the contaminants on the ceramic membrane surface were significantly alleviated and the membrane surface became porous, which improved the filtration performance and mitigated membrane fouling. In addition, as shown in Fig. 9d–f, the structure of ceramic membrane was mainly composed of porous support layer and surface separation layer. Compared with the cross-section of the original ceramic membrane, the separation layer of the polluted ceramic membrane trapped many contaminants, blocking the membrane pores and surface, resulting in membrane fouling. After pre-oxidation, the contaminants in the separation layer almost disappeared, which indicated that $O_3/TiO_2$ pre-oxidation could significantly degrade NOM and mitigate membrane fouling. In addition, the results of EDS (Fig. 10) also showed
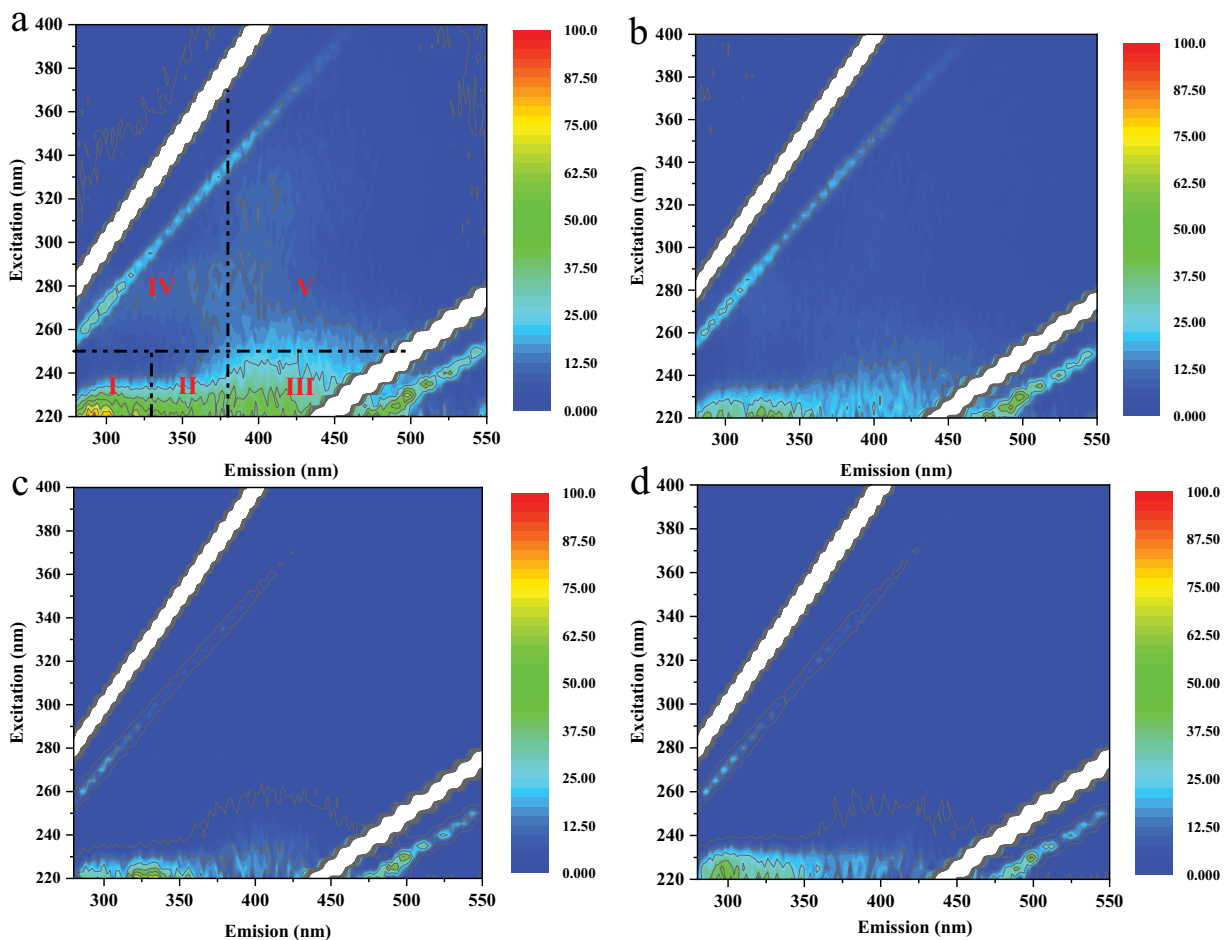


Fig. 7. Effects of different filtration models on the excitation–emission matrices of chemical cleaning solutions. (a) CMF, (b) $O_3$-CMF, (c) $O_3/H_2O_2$-CMF, and (d) $O_3/TiO_2$-CMF.
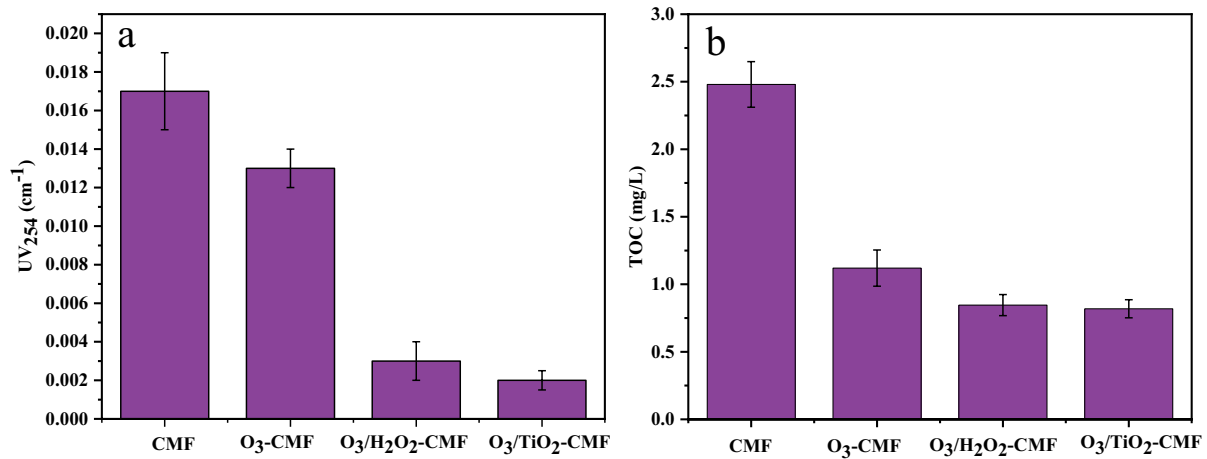
Fig. 8. Effects of different filtration models on the $UV_{254}$ (a) and TOC (b) of the chemical cleaning solutions
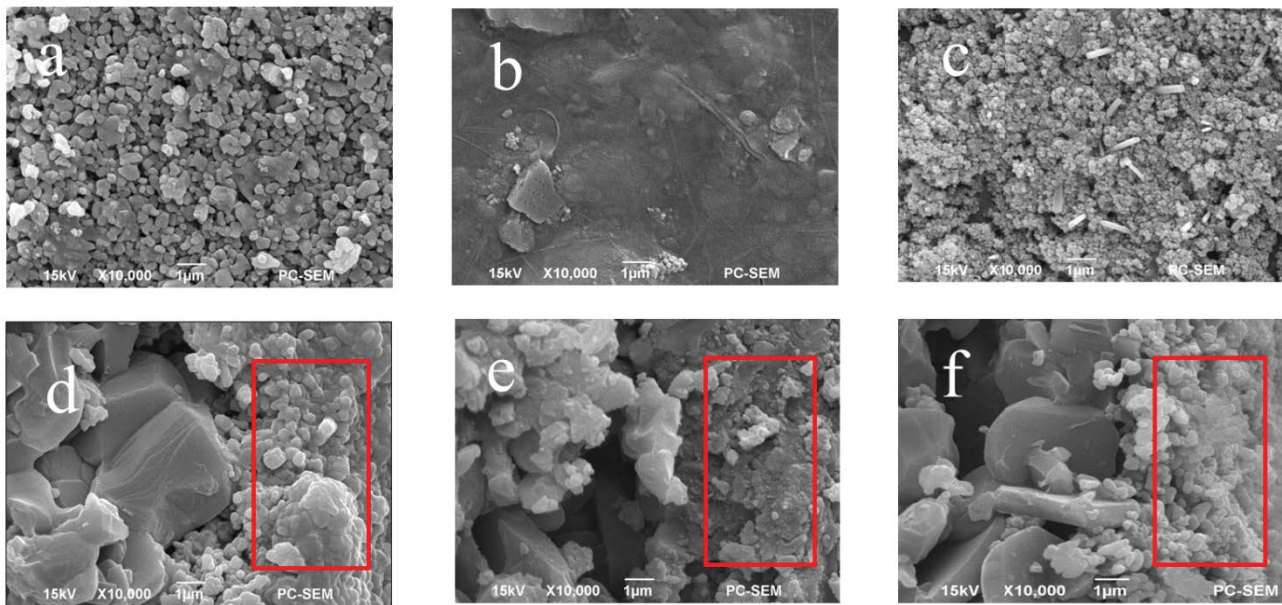


Fig. 9. Scanning electron microscopy images of ceramic membrane surface and cross-section. (a,d) Clean ceramic membrane, (b,e) ceramic membrane of CMF for 48 h, and (c,f) ceramic membrane of $O_3/TiO_2$-CMF for 48 h.

that compared with clean ceramic membrane, some usually found elements in the surface waters, such as Na, Mg, Si, Cl, Ca, Ti and Fe, were newly observed on the surface of ceramic membrane after 48 h filtration of CMF. However, after the filtration of $O_3/TiO_2$-CMF, the Fe element disappeared on the surface of ceramic membrane, and the proportion of Si element decreased significantly.

Fig. 11 shows the FTIR of the surface contaminants of the ceramic membrane after 48 h filtration of control, CMF and $O_3/TiO_2$-CMF, with the peak assignment in Table 2. It was obvious that after $O_3/TiO_2$ pre-oxidation, the strength of functional groups of O–H, C–H, –CH$_2$, C=C, C=O and C–O decreased significantly, and those of aromatic C–H, C–O, O–H and some aromatic rings C=C and C=O almost disappeared. The results further indicated that TiO$_2$ catalytic ozone destroyed benzene ring and double bonds, which

revealed that $O_3/TiO_2$ pre-oxidation could efficiently remove many organic compounds such as aromatic hydrocarbons, alkanes and carboxylic esters, thus mitigating the membrane fouling.

### 3.5. Redundancy analysis of membrane fouling

Generally, membrane fouling refers to unacceptable deposits on pores and surfaces of membrane. During the mass transfer process, the retentate was accumulated, adsorbed and adhered on the membrane surface or inside the membrane pores, and gradually formed a filter cake layer or gel layer on the membrane surface or in the pores over time [39]. The main causes for membrane fouling were organic matters, inorganic components, and microorganisms [40]. Particles were accumulated on the membrane surface
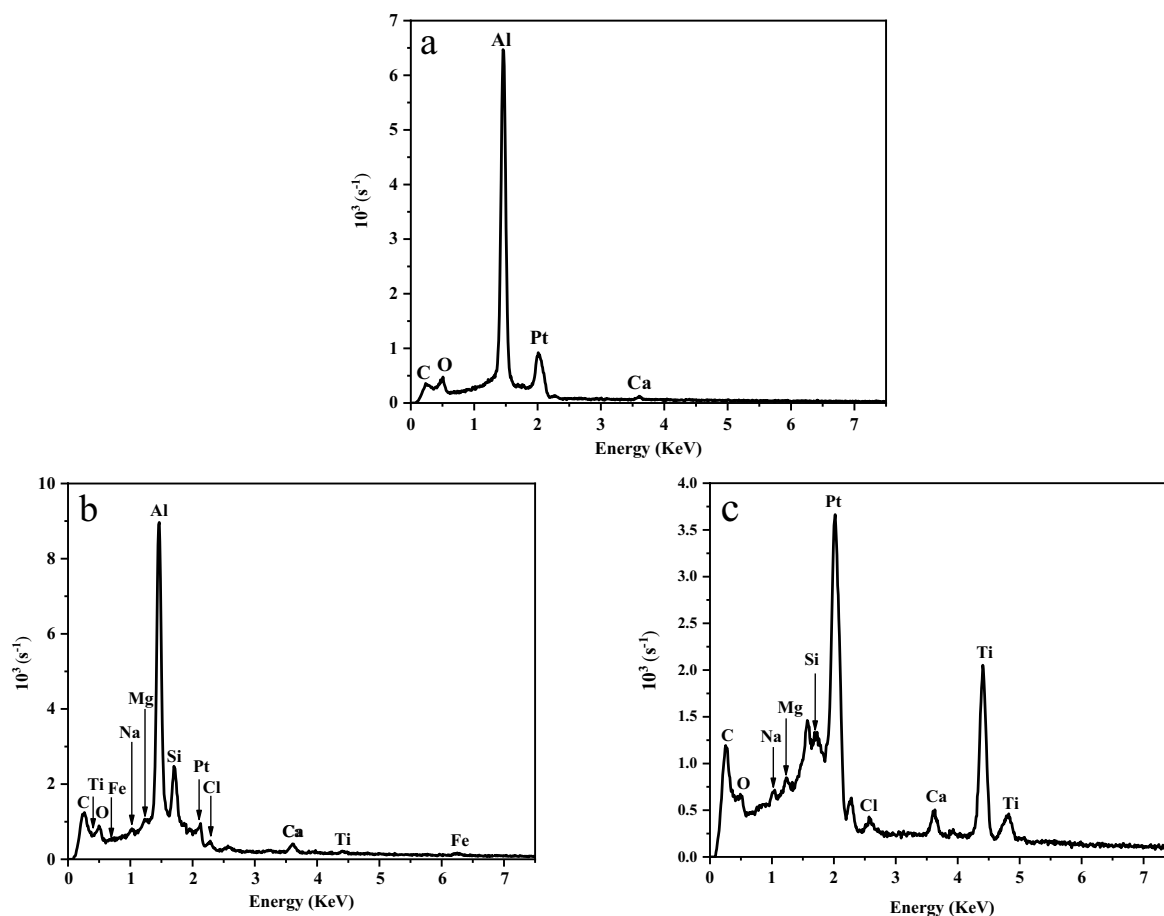
Fig. 10. Energy-dispersive X-ray spectroscopy of ceramic membrane surface. (a) Original ceramic membrane, (b) ceramic membrane of CMF filtration for 48 h, and (c) ceramic membrane of $O_3/TiO_2$-CMF filtration for 48 h.
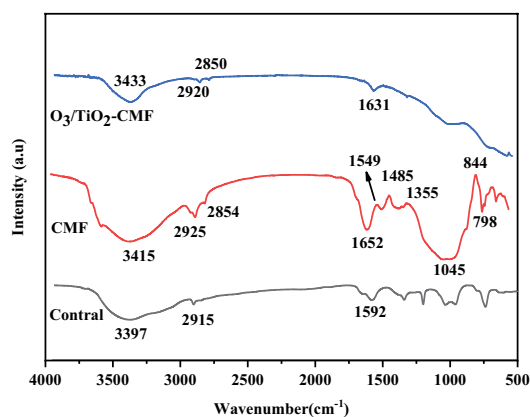


Fig. 11. Fourier-transform infrared spectroscopy diagram of the surface contaminants of the ceramic membrane after 48 h filtration of control, CMF and $O_3/TiO_2$-CMF.

Table 2
Peak assignment of Fourier-transform infrared spectra

| Absorption peak position ($cm^{-1}$) | Assignment |
| --- | --- |
| 3,397; 3,433; 3,415 | O–H in carboxyl and phenol |
| 2,915; 2,925; 2,920 | Aliphatic functional group C–H |
| 2,850; 2,854 | –$CH_2$ |
| 1,652; 1,631; 1,592; | Aromatic rings C=C and C=O |
| 1,549; 1,485 | (carbonyl, quinone, ester or carboxyl) |
| 1,400~1,000 | C–O (hydroxyl, ester, or ether) and O–H (phenolic) |
| 777~870 | Aromatic C–H |

forming a filter cake layer, and the organic and inorganic matters were adsorbed on the membrane holes forming gel layer. Three-dimensional fluorescence spectra and molecular weight distribution showed that humic acids and biopolymers were the main substances responsible for the membrane fouling. The pre-oxidation of $O_3$, $O_3/H_2O_2$ and $O_3/$ TiO$_2$ significantly mitigated the membrane fouling by degradation humic acids and biopolymers.

The pre-oxidation of $O_3$, $O_3/H_2O_2$ and $O_3/TiO_2$ significantly removed NOM and decreased the concentrations of TOC and $UV_{254}$ in surface water. The EEM spectra showed that the raw water and the CMF effluent were characterized with obvious fulvic acid-like substances, SMP and humic-like substances (Fig. 3). After pre-oxidation, the fluorescence intensity of each region decreased obviously, which indicated
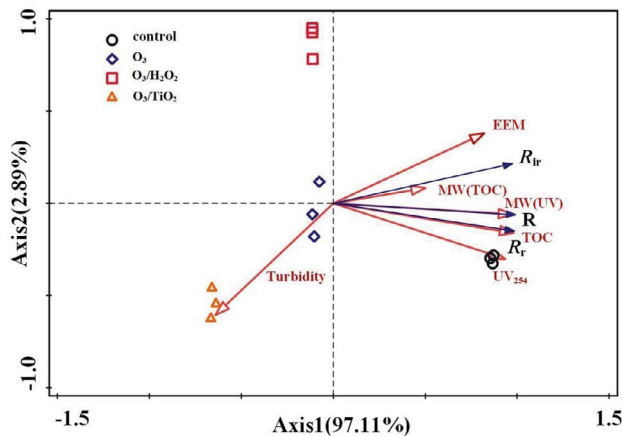
Fig. 12. Redundancy analysis of membrane fouling resistance and influent water characteristics for $O_3$, $O_3/H_2O_2$ and $O_3/TiO_2$ pre-oxidation.

that the organic matter was removed significantly. The raw surface water included biopolymers (20,000–200,000 Da), humic acid-like substances (350–20,000 Da), and low molecular weight organics (<350 Da) (Fig. 4). The peak intensities of biopolymer were significantly decreased after ceramic membrane filtration, which indicated that ceramic membrane could remove high molecular weight organic compounds [41]. The pre-oxidation of $O_3$, $O_3/H_2O_2$ and $O_3/TiO_2$ significantly mitigated the membrane fouling. Under $O_3/TiO_2$ pre-oxidation, the maximum TMP was reduced by 62.2% (Fig. 6a).

RDA was used to further clarify the correlation between membrane fouling resistance (total resistance, reversible resistance and irreversible resistance) and influent water characteristics [EEM, MW (TOC), MW (UV), TOC, $UV_{254}$, turbidity]. As shown in Fig. 12, the first and second axes of the RDA explained 97.11% and 2.89% of the total variance. The five parameters of EEM, MW (TOC), MW (UV), TOC and $UV_{254}$ were positively correlated with membrane fouling resistance, while the turbidity exhibited a negative correlation, which was consistent with previous studies [42]. It can be seen that after $O_3$, $O_3/H_2O_2$ and $O_3/TiO_2$ pre-oxidation, the membrane fouling mitigating was mainly due to the rapid decrease of organic matter and the improvement of water quality (Figs. 2–4). In addition, compared with $O_3$ and $O_3/H_2O_2$, $O_3/TiO_2$ pre-oxidation exhibited the efficient effect on fouling mitigation (Figs. 6–8). The reason might be that the nano $TiO_2$ could rapidly promote ozone decomposition to produce $^{\bullet}OH$. As shown in Fig. 12, $R_r$ was positively correlated with TOC, which indicated that the decrease of TOC led to the alleviation of reversible fouling resistance.

Results on the TOC, $UV_{254}$ and EEM of chemical cleaning solutions (Figs. 7 and 8) showed the low concentrations of organic matter, indicating the slight membrane fouling. This may be due partly to the fact that this study was performed in the batch model with short running time. In the long-term membrane fouling experiments, an enhanced removal of NOM as well as the mitigated membrane fouling were also observed by $O_3$, $O_3/H_2O_2$ and $O_3/TiO_2$ pre-oxidation.

## 4. Conclusion

This study systematically investigated the pre-oxidation coupled with ceramic membrane filtration for NOM removal and membrane fouling mitigating in surface water treatment. The main conclusions are as follows:

- After $O_3$, $O_3/H_2O_2$ and $O_3/TiO_2$ pre-oxidation, the NOM was degraded via direct and indirect oxidation, with a high decrease in TOC, $UV_{254}$, and SUVA, etc. The removal efficiencies for NOM decreased in the order of $O_3/TiO_2 > O_3/H_2O_2 > O_3$.
- Under the $O_3/TiO_2$ pre-oxidation, the fluorescence intensity of aromatic proteins, fulvic acid-like substances and humic-like substances even disappeared, leaving a small amount of SMP. The removed organic matter was mainly medium and high molecular weight organic matters, including humus and biopolymer. Three-dimensional fluorescence spectra and molecular weight distribution showed that humic acid and biopolymer were the main substances responsible for membrane fouling. The pre-oxidation of $O_3$, $O_3/H_2O_2$ and $O_3/TiO_2$ significantly mitigated the membrane fouling by degradation humic acids and biopolymers.
- The pre-oxidation of $O_3$, $O_3/H_2O_2$ and $O_3/TiO_2$ significantly mitigated the membrane fouling with the order of $O_3/TiO_2 > O_3/H_2O_2 > O_3$. Under optimal pre-oxidation, TMP was reduced by 62.2%.
- MW (UV) was the most important positive correlation factor for $R$ while turbidity was negatively correlated with $R$. The redundant results showed that the membrane fouling mitigating was mainly attributable to the degradation of organic matter.
- The long-term membrane fouling experiment also proved that the pre-oxidation coupled with ceramic membranes could effectively remove NOM in surface water and mitigate membrane fouling.

## Conflict-of-interest statement

The authors declare that we have no known competing financial interests or personal relationships that could have appeared to influence the work reported in this paper.

## Author contributions

Keying Li: experimental research and writing—original draft. Yong Wei: supervision, manuscript revision. Ming Kong: review and editing. Ziyin Guo: water quality analysis. Zhengbo Luo: data processing. Xianjian Li: device running. Rongkai Shi: project administration.

## References

[1] N.A. Wall, G.R. Choppin, Humic acids coagulation: influence of divalent cations, Appl. Geochem., 18 (2003) 1573–1582.

[2] N. Pathak, S. Li , Y. Kim, L. Chekli, S. Phuntsho, A. Jang, N. Ghaffour, T. Leiknes, H.K. Shon, Assessing the removal of organic micropollutants by a novel baffled osmotic membrane bioreactor-microfiltration hybrid system, Bioresour. Technol., 262 (2018) 98–106.

[3] W. Tang, G. Zeng, J. Gong, J. Liang, P. Xu, C. Zhang, B. Huang, Impact of humic/fulvic acid on the removal of heavy metals from aqueous solutions using nanomaterials: a review, Sci. Total Environ., 468–469 (2014) 1014–1027.

[4] Q, Zheng, X. Yang, W. Deng, X.C. Le, X. Li, Characterization of natural organic matter in water for optimizing water treatment and minimizing disinfection by-product formation, J. Environ. Sci., 42 (2016) 1–5.

[5] K. Kim, A. Jang, Evaluation of natural organic matter adsorption on Fe-Al binary oxide: comparison with single metal oxides, Chemosphere, 185 (2017) 247–257.

[6] S. Jia, Z. Yang, K. Ren, Z. Tian, C. Dong, R. Ma, G. Yu, W. Yang, Removal of antibiotics from water in the coexistence of suspended particles and natural organic matters using amino-acid-modified-chitosan flocculants: a combined experimental and theoretical study, J. Hazard. Mater., 317 (2016) 593–601.

[7] D. Lee, Y. Cheng, R. Wong, X. Wang, Adsorption removal of natural organic matters in waters using biochar, Bioresour. Technol., 260 (2018) 413–416.

[8] C. Liu, X. Tang, J. Kim, G.V. Korshin, Formation of aldehydes and carboxylic acids in ozonated surface water and wastewater: a clear relationship with fluorescence changes, Chemosphere, 125 (2015) 182–190.

[9] B. Liu, J. Yin, J. Wu, X. Cheng, K. Yang, G. Li, Z. Shi, Effect of $UV/ClO_2$ pretreatment on controlling ultrafiltration membrane fouling of different natural organic matter (NOM) fractions, J. Water Process Eng., 49 (2022) 103156, doi: 10.1016/j.jwpe.2022.103156.

[10] Y. Liu, J. Zhang, Recent research progress on reaction mechanism and influencing factors of $UV/H_2O_2$ advanced oxidation process, Chem. Ind. Eng. Technol., 32 (2011) 18–24.

[11] A. Tubić, J. Agbaba, B. Dalmacij, S.U. Perović, M. Klašnja, S. Rončević, I. Ivančev-Tumbas, Removal of natural organic matter from groundwater using advanced oxidation processes at a pilot scale drinking water treatment plant in the Central Banat Region (Serbia), Ozone Sci. Eng., 33 (2011) 267–278.

[12] H.A. Hasan, M.H. Muhammad, N. Ismail, A review of biological drinking water treatment technologies for contaminants removal from polluted water resources, J. Water Process Eng., 33 (2020) 101035, doi: 10.1016/j.jwpe.2019.101035.

[13] L. Deng, H. Ngo, W. Guo, H. Zhang, Pre-coagulation coupled with sponge-membrane filtration for organic matter removal and membrane fouling control during drinking water treatment, Water Res., 157 (2019) 155–166.

[14] J. Zhou, Y. Xia, Y. Gong, W. Li, Z. Li, Efficient natural organic matter removal from water using nano-MgO coupled with microfiltration membrane separation, Sci. Total Environ., 711 (2019) 135120, doi: 10.1016/j.scitotenv.2019.135120.

[15] X. Cheng, H. Liang, A. Ding, F. Qu, S. Shao, B. Liu, H. Wang, D. Wu, G. Li, Effects of pre-ozonation on the ultrafiltration of different natural organic matter (NOM) fractions: membrane fouling mitigation, prediction and mechanism, J. Membr. Sci., 505 (2016) 15–25.

[16] W. Huang, W. Lv, W. Zhou, M. Hu, B. Dong, Investigation of the fouling behaviors correlating to water characteristics during the ultrafiltration with ozone treatment, Sci. Total Environ., 676 (2019) 53–61.

[17] S. Robinson, S.Z. Abdullah, P. Bérubé, P. Le-Clech, Ageing of membranes for water treatment: linking changes to performance, J. Membr. Sci., 503 (2016) 177–187.

[18] Y. Rasouli, M. Abbasi, S.A. Hashemifard, Investigation of in-line coagulation-MF hybrid process for oily wastewater treatment by using novel ceramic membranes, J. Cleaner Prod., 161 (2017) 545–559.

[19] B. Düppenbecker, M. Engelhart, P. Cornel, Fouling mitigation in anaerobic membrane bioreactor using fluidized glass beads: evaluation fitness for purpose of ceramic membranes, J. Membr. Sci., 537 (2017) 69–82.

[20] S. Lee, J. Kim, Differential natural organic matter fouling of ceramic versus polymeric ultrafiltration membranes, Water Res., 48 (2014) 43–51.

[21] S. Tang, Z. Zhang, J. Liu, X. Zhang, Double-win effects of in-situ ozonation on improved filterability of mixed liquor and ceramic UF membrane fouling mitigation in wastewater treatment?, J. Membr. Sci., 533 (2017) 112–120.

[22] W. Chen, P. Westerhoff, J.A. Leenheer, K. Booksh, Fluorescence excitation-emission matrix regional integration to quantify spectra for dissolved organic matter, Environ. Sci. Technol., 37 (2003) 5701–5710.

[23] C. Lin, Y. Lin, P.S. Chandana, C. Tsai, Effects of mass retention of dissolved organic matter and membrane pore size on membrane fouling and flux decline, Water Res., 43 (2009) 389–394.

[24] R.F. Dantas, S. Contreras, C. Sans, S. Esplugas, Sulfamethoxazole abatement by means of ozonation, J. Hazard. Mater., 150 (2008) 790–794.

[25] H. Wang, S. Zhang, X. He, Y. Yang, X. Yang, W.H. Van Hulle, Comparison of macro and micro-pollutants abatement from biotreated landfill leachate by single ozonation, $O_3/H_2O_2$, and catalytic ozonation processes, Chem. Eng. J., 452 (2023) 139503, doi: 10.1016/j.cej.2022.139503.

[26] C. Hai, J. Wang, Degradation and mineralization of ofloxacin by ozonation and peroxone ($O_3/H_2O_2$) process, Chemosphere, 269 (2021) 128775, doi: 10.1016/j.chemosphere.2020.128775.

[27] J. Nawrocki, L. Fijołek, Effect of aluminium oxide contaminants on the process of ozone decomposition in water, Appl. Catal., B, 142 (2013) 533–537.

[28] S.A. Baghoth, S.K. Sharma, G.L. Amy, Tracking natural organic matter (NOM) in a drinking water treatment plant using fluorescence excitation–emission matrices and PARAFAC, Water Res., 45 (2011) 797–809.

[29] S.A. Huber, A. Balz, M. Abert, W. Pronk, Characterisation of aquatic humic and non-humic matter with size-exclusion chromatography – organic carbon detection – organic nitrogen detection (LC-OCD-OND), Water Res., 45 (2011) 879–885.

[30] M. Sillanpää, M.C. Ncibi, A. Matilainen, Advanced oxidation processes for the removal of natural organic matter from drinking water sources: a comprehensive review, J. Environ. Manage., 208 (2018) 56–76.

[31] C. Mansas, J. Mendret, S. Brosillon, A. Ayral, Coupling catalytic ozonation and membrane separation: a review, Sep. Purif. Technol., 236 (2020) 116221, doi: 10.1016/j.seppur.2019.116221.

[32] P.L. Clech, B. Jefferson, I.S. Chang, S.J. Judd, Critical flux determination by the flux-step method in a submerged membrane bioreactor, J. Membr. Sci., 227 (2003) 81–93.

[33] X. Zhang, X. Yue, Z. Liu, Q. Li, X. Hua, Impacts of sludge retention time on sludge characteristics and membrane fouling in a submerged anaerobic–oxic membrane bioreactor, Appl. Microbiol. Biotechnol., 99 (2015) 4893–4903.

[34] H. Park, Y. Kim, B. An, H. Choi, Characterization of natural organic matter treated by iron oxide nanoparticle incorporated ceramic membrane-ozonation process, Water Res., 46 (2012) 5861–5870.

[35] K. Szymanska, A.I. Zouboulis, D. Zamboulis, Hybrid ozonation–microfiltration system for the treatment of surface water using ceramic membrane, J. Membr. Sci., 468 (2014) 163–171.

[36] C. Chen, P. Fang, K. Chen, Permeate flux recovery of ceramic membrane using $TiO_2$ with catalytic ozonation, Ceram. Int., 43 (2017) 758–764.

[37] Z. Wang, Y. Wan, P. Xie, A. Zhou, J. Ding, J. Wang, L. Zhang, S. Wang, T.C. Zhang, Ultraviolet/persulfate (UV/PS) pretreatment of typical natural organic matter (NOM): variation of characteristics and control of membrane fouling, Chemosphere, 214 (2019) 136–147.

[38] X. Cheng, D. Wu, H. Liang, X. Zhu, X. Tang, Z. Gan, J. Xing, X. Luo, G. Li, Effect of sulfate radical-based oxidation

pretreatments for mitigating ceramic UF membrane fouling caused by algal extracellular organic matter, Water Res., 145 (2018) 39–49.

[39] X. Shi, G. Tal, N.P. Hankins, V. Gitis, Fouling and cleaning of ultrafiltration membranes: a review, J. Water Process Eng., 1 (2014) 121–138.

[40] J. Saqib, I.H. Aljundi, Membrane fouling and modification using surface treatment and layer-by-layer assembly of polyelectrolytes: state-of-the-art review, J. Water Process Eng., 11 (2016) 68–87.

[41] D. Wei, Y. Tao, Z. Zhang, L. Liu, X. Zhang, Effect of in-situ ozonation on ceramic UF membrane fouling mitigation in algal-rich water treatment, J. Membr. Sci., 498 (2016) 116–124.

[42] J. Liu, K. He, S. Tang, T. Wang, Z. Zhang, A comparative study of ferrous, ferric and ferrate pretreatment for ceramic membrane fouling alleviation in reclaimed water treatment, Sep. Purif. Technol., 217 (2019) 118–127.